

Green CoO-NPS-Catalyzed Synthesis, Spectral Analysis, And Antimicrobial Assessment Of 5-Amino-1,3-Diphenyl-1h-Pyrazole-4-Carbonitrile Derivatives

Amol R. Pagare¹, Rajashri B. Sawant^{2*}, Vivek Patil³, Somnath S. Gholap¹

¹Dept of Chem, Arts, Science, and Commerce College Rahata, Pimplas (Rahata), Ahmednagar, Maharashtra India

²Dept of Chem, M.P.H. Arts, Science, and Commerce Mahila College, Malegaon Camp, Nashik, Maharashtra, rajashriahire@gmail.com

³Dept of Chemistry, Swami Muktanand College of Science, Yeola, Maharashtra, India.

In this study, we investigate the utilization of Green CoO-NPs as a catalyst in synthesizing 5-amino-1,3-diphenyl-1H-pyrazole-4-carbonitrile derivatives, alongside the environmentally sustainable method of producing CoO particles. The characterization of bio-derived CoO particles was performed using X-ray diffraction (XRD), energy-dispersive X-ray spectroscopy (EDAX), Fourier-transform infrared spectroscopy (FTIR), and ultraviolet-visible spectroscopy (UV). Chalcones were synthesized as antimicrobial agents through the Claisen-Schmidt condensation of malonitrile and phenylhydrazine with various aromatic aldehydes, employing BuniumPersicum extracted CoO-NPs as the catalyst.

The synthesized 5-amino-1,3-diphenyl-1H-pyrazole-4-carbonitrile derivatives were identified and characterized using UV, FT-IR, mass spectrometry, proton nuclear magnetic resonance (¹H-NMR) spectroscopy, and elemental analysis. Notably, the one-step condensation of substituted aryl carbonyls facilitated the rapid synthesis of substituted chalcones in under three minutes under solvent-free conditions, assisted by microwave irradiation, yielding 90-93%.

The significant advantages of our methodology include the reduced reaction time and the high yield of substituted chalcones. The antimicrobial and antifungal properties of the synthesized 5-amino-1,3-diphenyl-1H-pyrazole-4-carbonitriles were evaluated using the disc diffusion method, and tested against two gram-positive and two gram-negative bacterial strains, as well as two fungal strains.

Keywords: 5-amino-1,3-diphenyl-1H-pyrazole-4-carbonitrile, BuniumPersicum, Antibacterial activity, Antifungal activity, Green synthesis.

1. Introduction

There has been a growing interest in developing eco-friendly products and processes due to concerns about climate change, water contamination, depletion of natural resources, human health, and related issues. Consequently, researchers have been exploring various methods to enhance the green synthesis of metal and metal oxide nanoparticles¹⁻³. Nanotechnology has opened new horizons in material science, particularly with the synthesis and application of metal oxide nanoparticles. Among these, cobalt oxide (CoO) nanoparticles have garnered significant attention due to their unique physicochemical properties and potential applications in catalysis⁴, energy storage⁵, magnetic materials⁶, and biomedical fields⁷. The green synthesis of CoO nanoparticles using plant extracts has emerged as an environmentally friendly and cost-effective alternative to conventional methods, which often involve toxic chemicals and high energy consumption⁸⁻⁹.

The green synthesis approach uses plant extracts as both reducing and stabilizing agents. This method leverages the natural phytochemicals present in plants, such as flavonoids, alkaloids, terpenoids, and polyphenols, which can reduce metal ions to their respective nanoparticles¹⁰⁻¹³. The process typically involves mixing an aqueous solution of cobalt salts with plant extracts under controlled conditions, leading to the formation of CoO nanoparticles¹⁴⁻¹⁶.

Various plant extracts have been employed in the synthesis of CoO nanoparticles¹⁷⁻²¹. The synthesized CoO nanoparticles are typically characterized using various analytical techniques: X-ray Diffraction (XRD), Scanning Electron Microscopy (SEM), Transmission Electron Microscopy (TEM), Fourier-Transform Infrared Spectroscopy (FTIR), UV-visible spectroscopy (UV-Vis), X-ray Photoelectron Spectroscopy (XPS). Plant-extracted CoO nanoparticles exhibit a range of applications due to their enhanced properties. CoO nanoparticles serve as effective catalysts in various chemical reactions, including the oxidation of organic pollutants and water splitting²². They are used in the fabrication of electrodes for supercapacitors and lithium-ion batteries, owing to their high specific capacitance and excellent electrochemical stability²³. CoO nanoparticles exhibit superparamagnetic properties, making them suitable for magnetic storage devices and magnetic resonance imaging (MRI) contrast agents²⁴. Their biocompatibility and antimicrobial properties make CoO nanoparticles useful in drug delivery systems, cancer therapy, and as antibacterial agents²⁵.

The green synthesis of CoO nanoparticles offers several advantages over traditional methods: Environmental Sustainability²⁶, Cost-Effectiveness²⁷, and Biocompatibility²⁸. The green synthesis of CoO nanoparticles using plant extracts represents a promising and sustainable approach to nanomaterial synthesis. With ongoing research and development, plant-extracted CoO nanoparticles are poised to play a significant role in catalysis, energy storage, magnetic materials, and biomedical applications, contributing to the advancement of nanotechnology and green chemistry.

Bunium persicum, commonly known as black cumin, is a highly valued medicinal plant in the Apiaceae family. Native to the Middle East and South Asia, black cumin is renowned for its rich phytochemical profile. It has been used for centuries in traditional medicine, culinary applications, and as a flavoring agent²⁹⁻³³. Black cumin seeds are a powerhouse of bioactive compounds, which include: Essential Oils, Alkaloids, Flavonoids, Saponins, and Tannins. The medicinal importance of *Bunium persicum* can be attributed to its diverse pharmacological

activities such as; Antimicrobial Activity³⁴, Anti-Inflammatory Effects³⁵, Digestive Health³⁶, Antidiabetic Potential³⁷, Cardioprotective Effects³⁸, Cancer Prevention³⁹, Culinary Uses⁴⁰, Agricultural and Economic Importance⁴¹, Crop Cultivation⁴² and Market Demand⁴³.

Buniumpersicum, or black cumin, is a plant of immense importance due to its rich phytochemical profile and versatile applications. Its medicinal properties, culinary uses, and economic significance underscore the need for further research and development. Promoting the cultivation and utilization of black cumin can contribute to health, agriculture, and the economy, making it a valuable asset in traditional and modern practices.

In this study, we employed *BuniumPersicum* extract to develop cobalt oxide (CoO) particles through an environmentally friendly and cost-effective process. This method avoids the use of harsh, harmful, and expensive chemicals, resulting in well-characterized nanoparticles produced in an eco-friendly manner. Furthermore, the cost-effectiveness of this procedure enhances its practicality. It has been reported that cobalt oxide (CoO) exhibits catalytic activity in the solvent-free microwave synthesis of 5-amino-1,3-diphenyl-1H-pyrazole-4-carbonitriles, in addition to its application in green synthesis.

2. Experimental:

The synthesis of 5-amino-1,3-diphenyl-1H-pyrazole-4-carbonitriles involved the utilization of *BuniumPersicum* extract and reagents obtained from BLD Pharma in India. Uncorrected melting points were determined using open capillary tubes. The FT-IR spectra were recorded in potassium bromide (KBr) using a Bruker Spectrophotometer. Proton nuclear magnetic resonance (¹H-NMR) spectra were obtained in deuterated chloroform (CDCl₃) with tetramethylsilane (TMS) as an internal standard, using a Bruker 400 MHz Spectrometer. Elemental analyses were carried out using a Carlo Erba 1108 elemental analyzer. The UV-visible spectra were acquired at room temperature in methanol using a JASCO V650 UV-visible spectrophotometer. Mass spectrometry analysis of the synthesized organic compounds was performed using Bruker IMPACT HD instruments. The purity of the compounds was verified by thin-layer chromatography (TLC) on Silica gel-G (Merck). X-ray diffraction (XRD) measurements were conducted using a Rigaku ULTIMA IV diffractometer with a Cu-K α X-ray source operating at a voltage of 40 kV. X-ray photoelectron spectroscopy (XPS) was performed using an ESCALAB 300 (Thermo-VG Scientific). These comprehensive analytical techniques ensured the accurate characterization and verification of the synthesized chalcone derivatives.

PREPARATION OF AQUEOUS BUNIUMPERSICUM EXTRACT:

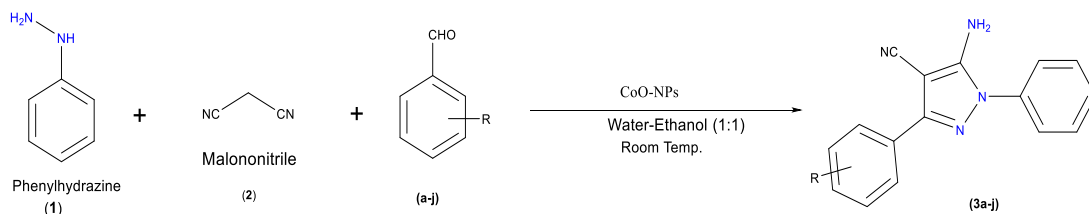
The *BuniumPersicum* seeds were collected and thoroughly washed with tap water followed by deionized water. To prepare the aqueous extract, 10 grams of the dry *BuniumPersicum* seeds, were mixed with 100 mL of deionized water in a 250 mL beaker. The mixture was heated to 60°C for 1 hour. After heating, the solution was cooled and filtered using Whatman No. 1 filter paper. The resulting filtrate was stored in an airtight container at room temperature for future experiments.

BIOSYNTHESIS OF COBALT OXIDE NANOPARTICLES:

The synthesis of cobalt oxide nanoparticles (CoO-NPs) was carried out by gradually adding BuniumPersicumseeds extract to a 100 mL conical flask containing a 0.01 mM $\text{CoCl}_2 \cdot 7\text{H}_2\text{O}$ solution while maintaining a constant agitation speed of 1000 rpm. The reaction mixture was agitated using a magnetic stirrer for 15 minutes at 30°C . Following this, the CoO-NPs were separated by centrifugation at 15,000 rpm for 20 minutes. To purify the nanoparticles, the centrifugation process was repeated multiple times, each time washing the solid pellet with triple distilled water to remove the liquid supernatant. The purified CoO-NPs were then freeze-dried at 0°C and 10 Pa for 24 hours. The resulting black pellet was dehydrated and stored for future research.

GENERAL PROCEDURE FOR THE PREPARATION OF 5-AMINO-1,3-DIPHENYL-1H-PYRAZOLE-4-CARBONITRILE DERIVATIVES:

In a 250 mL round-bottomed flask, aromatic aldehyde (1 mol), malonitrile (1 mol), phenylhydrazine (1 mol), and CoO-NPs (10 mol%) were added to a 50 mL mixture of water and ethanol (1:1) at room temperature. The mixture was then subjected to microwave irradiation. The reaction progress was monitored by thin-layer chromatography (TLC). Upon completion, the product crystallized out of the reaction mixture. These crystals were collected by filtration and recrystallized from ethanol to obtain the pure product (Scheme 1).



Scheme 1: Greener Synthesis of 5-amino-3-aryl-1-phenyl-1H-pyrazole-4-carbonitrile from phenylhydrazine, malononitrile, and substituted benzaldehydes

Selected spectral data of the products:

5-Amino-3-(2,4-dihydroxyphenyl)-1-phenyl-1H-pyrazole-4-carbonitrile (3a): Yellow powder (91.17 %), M.P. = 178°C , FT(IR) spectrum (KBr) 3320, 2951, 2205, 1685, 1599, 1444, 1249, 736, 684 cm^{-1} . ^1H NMR (CDCl_3 , 500 MHz): δ (ppm) 10.20 (s, 1H), 7.85 (s, 1H), 7.35 (d, 2H), 6.74-7.34 (m, 8H). UV spectrum (λ_{nm}) 325, 281. MS (m/z): 289.68 (M^+). (Anal. Calcd for $\text{C}_{16}\text{H}_{12}\text{N}_4\text{O}_2$: C, 65.75; H, 4.14; N, 19.17; O, 10.95 %. Found: C, 65.47; H, 4.07; N, 18.76, O, 10.93 %.

5-Amino-3-(2,3-dimethoxyphenyl)-1-phenyl-1H-pyrazole-4-carbonitrile (3b): White powder (94.99 %), M.P. = 127°C , FT(IR) spectrum (KBr) 3293, 2239, 1686, 1249, 735, 685 cm^{-1} . ^1H NMR (CDCl_3 , 500 MHz): δ (ppm) 7.61 (d, 2H), 7.63 (d, 2H), 6.87-7.59 (m, 8H), 3.94-4.02 (s, 6H). UV spectrum (λ_{nm}) 356, 271. MS (m/z): 322.99 (M^+). (Anal. Calcd for $\text{C}_{18}\text{H}_{16}\text{N}_4\text{O}_2$: C, 67.49; H, 5.03; N, 19.49; O, 9.99 %. Found: C, 66.38; H, 4.98; N, 19.41, O, 9.92 %.

5-Amino-3-(2-hydroxy-4-methoxyphenyl)-1-phenyl-1H-pyrazole-4-carbonitrile (3c): White powder (93.61 %), M.P. = 155 °C, FT(IR) spectrum (KBr) 3407, 3291, 2211, 1596, 1252, 734, 688 cm^{-1} . ^1H NMR (CDCl_3 , 500 MHz): δ (ppm) 5.85 (s, 1H), 4.27-4.28 (d, 2H), 6.89-7.66 (m, 8H), 1.50-1.54 (s, 3H). UV spectrum (λ_{nm}) 362, 278. MS (m/z): 301.16 (M) $^+$. (Anal. Calcd for $\text{C}_{17}\text{H}_{14}\text{N}_4\text{O}_2$: C, 66.66; H, 4.61; N, 18.29; O, 10.45 %. Found: C, 66.61; H, 4.59; N, 18.21, O, 10.38 %.

5-Amino-3-(3,5-dichloro-6-hydroxyphenyl)-1-phenyl-1H-pyrazole-4-carbonitrile (3d): White powder (90.00 %), M.P. = 161 °C, FT(IR) spectrum (KBr) 3443, 3338/3294, 2192, 1644, 1252, 733, 691 cm^{-1} . ^1H NMR (CDCl_3 , 500 MHz): δ (ppm) 11.55 (s, 1H), 7.65-7.68 (d, 2H), 6.93-7.31 (m, 7H). UV spectrum (λ_{nm}) 382, 317. MS (m/z): 338.77 (M) $^+$. (Anal. Calcd for $\text{C}_{16}\text{H}_{10}\text{N}_4\text{OCl}_2$: C, 55.67; H, 2.92; N, 16.23; O, 4.64; Cl, 29.34 %. Found: C, 55.62; H, 2.88; N, 16.15, O, 4.21; Cl, 29.27 %.

5-Amino-3-(3-ethoxy-4-methoxyphenyl)-1-phenyl-1H-pyrazole-4-carbonitrile (3e): Red-brown powder (90.36 %), M.P. = 170 °C, FT(IR) spectrum (KBr) 3327, 2191, 1598, 1251, 743, 688 cm^{-1} . ^1H NMR (CDCl_3 , 500 MHz): δ (ppm) 11.77 (s, 1H), 8.17 (d, 2H), 7.30-7.92 (m, 7H), 7.01-7.10 (s, 5H), 3.56 (s, 3H). UV spectrum (λ_{nm}) 333, 272. MS (m/z): 332.91 (M) $^+$. (Anal. Calcd for $\text{C}_{19}\text{H}_{18}\text{N}_4\text{O}_2$: C, 68.25; H, 5.43; N, 16.76; O, 9.57%. Found: C, 68.02; H, 5.33; N, 16.10, O, 9.48%.

5-Amino-3-(3,4-dibromophenyl)-1-phenyl-1H-pyrazole-4-carbonitrile (3f): Yellow powder (95.00 %), M.P. = 177 °C, FT(IR) spectrum (KBr) 3305, 1923, 1588, 1251, 748, 652, 631 cm^{-1} . ^1H NMR (CDCl_3 , 500 MHz): δ (ppm) 7.47-7.91 (d, 2H), 6.93-7.74 (m, 8H). UV spectrum (λ_{nm}) 329, 273. MS (m/z): 417.00 (M) $^+$. (Anal. Calcd for $\text{C}_{16}\text{H}_{10}\text{N}_4\text{Br}_2$: C, 45.96; H, 2.41; N, 13.40; Br, 38.22 %. Found: C, 45.66; H, 2.33; N, 13.21; Br, 38.16 %.

5-Amino-3-(2, 5-dibromophenyl)-1-phenyl-1H-pyrazole-4-carbonitrile (3g): Yellow powder (94.40 %), M.P. = 176 °C, FT(IR) spectrum (KBr) 3302, 2216, 1563, 1252, 752, 693, 635 cm^{-1} . ^1H NMR (CDCl_3 , 500 MHz): δ (ppm) 8.20 (d, 2H), 6.95-7.96 (m, 8H). UV spectrum (λ_{nm}) 337, 309. MS (m/z): 420.95 (M) $^+$. (Anal. Calcd for $\text{C}_{16}\text{H}_{10}\text{N}_4\text{Br}_2$: C, 45.96; H, 2.41; N, 13.40; Br, 38.22 %. Found: C, 45.91; H, 2.37; N, 13.27; Br, 38.19 %.

5-Amino-3-(3,4-difluorophenyl)-1-phenyl-1H-pyrazole-4-carbonitrile (3h): Yellow powder (93.57 %), M.P. = 149 °C, FT(IR) spectrum (KBr) 3303, 2236, 1595, 1248, 1249, 752, 691 cm^{-1} . ^1H NMR (CDCl_3 , 500 MHz): δ (ppm) 7.54-7.63 (d, 2H), 6.86-7.54 (m, 8H). UV spectrum (λ_{nm}) 336. MS (m/z): 297.33 (M) $^+$. (Anal. Calcd for $\text{C}_{16}\text{H}_{10}\text{N}_4\text{Cl}_2$: C, 64.86; H, 3.40; N, 12.62; F, 18.91 %. Found: C, 64.80; H, 3.33; N, 12.55; F, 18.85 %.

5-Amino-3-(2,5-difluorophenyl)-1-phenyl-1H-pyrazole-4-carbonitrile (3i): Yellow powder (91.85 %), M.P. = 150 °C, FT(IR) spectrum (KBr) 3251, 2211, 1595, 1249, 1239, 745, 689 cm^{-1} . ^1H NMR (CDCl_3 , 500 MHz): δ (ppm) 7.68 (d, 2H), 6.95-7.75 (m, 8H). UV spectrum (λ_{nm}) 333, 287. MS (m/z): 297.08 (M) $^+$. (Anal. Calcd for $\text{C}_{16}\text{H}_{10}\text{N}_4\text{Cl}_2$: C, 64.86; H, 3.40; N, 12.62; F, 18.91 %. Found: C, 64.83; H, 3.36; N, 12.57; F, 18.88 %.

5-Amino-3-(2,4-dibromophenyl)-1-phenyl-1H-pyrazole-4-carbonitrile (3j): Yellow powder (90.51 %), M.P. = 168 °C, FT(IR) spectrum (KBr) 3396, 2208, 1599, 1247, 750, 693, 639 cm^{-1} . ^1H NMR (CDCl_3 , 500 MHz): δ (ppm) 7.96 (d, 2H), 6.95-7.89 (m, 8H). UV spectrum (λ_{nm}) 317. MS (m/z): 428.96 (M) $^+$. (Anal. Calcd for $\text{C}_{16}\text{H}_{10}\text{N}_4\text{Br}_2$: C, 45.96; H, 2.41; N, 13.40; Br, 38.22 %. Found: C, 45.93; H, 2.37; N, 13.39; Br, 38.19 %.

ANTIMICROBIAL ACTIVITY:

To assess antimicrobial activity, we used synthetic compounds against a variety of fungal and bacterial clinical isolates, which were purchased as dry powder. The fungal strains included *Candida albicans* MCC1439 and *Saccharomyces cerevisiae* MCC1033. Mold isolates were maintained in sterile water to ensure vitality and purity before being sub-cultured on antimicrobial agent-free potato dextrose agar. The bacterial strains included Gram-negative *Escherichia coli* MCC2412 and *Pseudomonas aeruginosa* MCC2080, and Gram-positive *Bacillus subtilis* MCC2010 and *Staphylococcus aureus* MCC2010. These organisms were obtained from the National Centre for Molecular Research in Pune, India.

Dimethyl formamide (DMF) was used to dissolve the compounds, which were then stored at 4°C, though no antibacterial activity was observed at the tested concentrations. Bacteria were cultured in nutrient broth (NB; Difco) and nutrient agar (NA), while fungi were grown in potato dextrose agar and Sabouraud liquid media.

ANTIBACTERIAL SCREENING:

To evaluate the antibacterial efficacy of the synthesized compounds, a panel of four bacteria was used: two Gram-positive (*S. aureus* MCC2010 and *B. subtilis* MCC2010) and two Gram-negative (*E. coli* MCC2412 and *P. aeruginosa* MCC2080). Muller Hilton agar medium was autoclaved at 15 lbs/in 2 for 15 minutes for antibacterial testing. The disc diffusion method was employed to assess antibacterial activity. The inoculum was diluted in sterile distilled water to approximately 10^8 cfu/mL. The desired microbial strains were introduced to 20 mL of Muller Hilton agar medium by swabbing it onto petri dishes. Wells of 6 mm diameter were bored into the pre-inoculated plates using a sterile borer, and 100 μL of a 4.0 mg/mL solution of each compound, reconstituted in DMSO, was added to each well. Plates were incubated at 37°C for 24 hours. Antibacterial activity was evaluated by measuring the zone of inhibition around the wells. Streptomycin and DMSO were used as control solvents⁴⁴⁻⁴⁵.

ANTIFUNGAL ACTIVITY:

The antifungal efficacy of the compounds was tested using the cup-and-plate method against *Candida albicans* MCC1439 and *Saccharomyces cerevisiae* MCC1033. Discs of 6 mm diameter and 1 mm thickness were impregnated with the test solutions using a micropipette. Plates were incubated at 37°C for 72 hours, and the effect of the experimental solution on fungal growth was assessed. The size of the inhibition zone was measured after 36 hours. Minimum inhibitory concentrations (MICs) of the compounds were determined, defined as the lowest concentration at which noticeable microbial growth was inhibited after overnight incubation. MIC values are crucial for confirming microbial resistance to existing antimicrobials and for evaluating the efficacy of new antimicrobial agents in clinical laboratories⁴⁶⁻⁴⁷.

3. Results and Discussion:

CHARACTERIZATION OF COBALT OXIDE NANOPARTICLES

Cobalt oxide (CoO) nanoparticle synthesis was evaluated and analyzed using standard instrumentation and techniques, adhering to environmentally conscious protocols. The formation of CoO nanoparticles was initially indicated by a color change in the reaction mixture. The presence and successful synthesis of cobalt oxide nanoparticles were confirmed through the analysis of data obtained from UV-visible (UV-vis) and Fourier-transform infrared (FTIR) spectroscopy.

XRD SPECTRAL ANALYSIS:

The phase purity of the products was determined under optimal experimental conditions. The powder XRD patterns of the synthesized iron oxide nanoparticles are shown in Figure 1. The patterns revealed the presence of the pure hematite Fe_2O_3 phase, which corresponds to PDF-01-077-9926. The primary hematite peak is distinctly observed at 33.24° , along with additional peaks identified at 24.24° , 35.74° , 40.56° , 49.56° , 54.18° , 57.68° (doublet), 62.50° , and 64.12° . Similarly, the powder XRD patterns of the CoO nanoparticles, illustrated in Figure 1, were analyzed. The diffraction peaks corresponding to the (111), (200), (220), (311), and (222) planes of face-centered cubic (fcc) CoO match the bulk XRD pattern (CoO, Fm3m, $a = 4.261 \text{ \AA}$, JCPDS #78-0431) and are observed at 2θ values of 36.36° , 44.96° , 59.44° , 65.30° , and 66.00° , respectively. There was no shift in the peak positions across the angular range of $20-80^\circ$, indicating that the synthesized cubic CoO nanocrystals are free from extraneous strain. Detailed structural characterization through least-squares refinement of the XRD patterns using the PowderCell program confirmed the as-synthesized material as crystalline pure phase CoO, with a calculated cell parameter $a = 4.262 \text{ \AA}$ and space group Fm3m. The XRD patterns confirmed the high purity of the synthesized products, as no additional phases such as Co_3O_4 , hexagonal $\beta\text{-Co(OH)}_2$, metallic cobalt (Co, JCPDS #05-0727), or hexagonal CoO (JCPDS #80-0075) were detected⁴⁸⁻⁵⁰.

FT-IR SPECTRAL ANALYSIS:

The FT-IR spectra of CoO nanoparticles, presented in Figure 2, were recorded in the $500-4000 \text{ cm}^{-1}$ spectral range. The prominent bands observed at 1633 cm^{-1} and 1347 cm^{-1} correspond to the carbonyl and C-N functional groups, respectively, as reported previously⁵¹. Additionally, the infrared spectra exhibit two distinct bands at $\sim 577 \text{ cm}^{-1}$, attributed to the $\nu(\text{Co-O})$ vibrational modes⁵². These modes originate from the characteristic stretching vibrations of the cobalt-oxygen bonds in CoO.

UV-Visible Spectral Analysis:

Figure 3 illustrates the UV-visible absorption spectrum of a pure CoO nanoparticle sample. The absorption edges are observed at wavelengths of 273 nm, 347 nm, and 363 nm. These absorption edges below 400 nm are attributed to charge transfer from the O 2p to the Co 3d states⁵³. The absorption spectrum of CoO nanoparticles exhibits a red shift toward higher wavelengths, indicating the incorporation of transition metals into the CoO nanoparticle lattice sites.

The optical band gaps (E_g) of pure CoO nanoparticles were determined using the Tauc plot

method, represented by the equation $\alpha h\nu = A(h\nu - E_g)^n$. The band gaps for CoO nanoparticles were found to be 3.73 eV, 3.58 eV, and 3.34 eV, respectively. The CoO nanoparticles exhibited a reduced band gap energy compared to their pure forms.

SEM ANALYSIS:

The surface morphology of pure CoO nanoparticles is depicted in Figure 4. The nanoparticles generally exhibit spherical shapes and are within the nanoscale range. The incorporation of Co ions into the lattice sites of CoO leads to the enlargement of small pores within these nanoparticles. The presence of transition metals in the structure was confirmed⁵⁴.

EDAX ANALYSIS:

The elemental composition of CoO nanoparticles was examined in this study using Energy-Dispersive X-ray Spectroscopy (EDAX). The results indicate that the concentration of Co^{2+} ion is 6.25%. Additionally, the analysis reveals that the CoO nanoparticles contain 60% oxygen atoms⁵⁵.

CATALYTIC SCREENING AND REACTION OPTIMIZATION:

The catalytic screening was conducted at room temperature using various catalysts, along with 1 mmol each of aromatic benzaldehyde, phenylhydrazine, and malononitrile. The results indicated that the type of catalyst had no significant impact on the yield of pyrazole derivatives. Notably, a base catalyst was unnecessary for achieving the desired 5-amino-4-cyanopyrazole derivatives, which were produced in remarkable yields after 2 min of reaction at room temperature in a solvent mixture of water and ethanol (1:1 v/v). Phenylhydrazine demonstrated dual functionality as both a nucleophile and a catalyst for the Brønsted base reaction, with bases not affecting the yield of the reaction. Further investigations showed that varying the concentration of phenylhydrazine did not significantly affect the yield of 5-amino-1,3-diphenyl-1H-pyrazole-4-carbonitrile, and decreasing its amount did not achieve total conversion.

Under these optimized conditions, the three-component reaction was successfully extended to include a diverse range of aromatic aldehydes, malononitrile, and phenylhydrazine derivatives. High product yields were consistently achieved, even with low nucleophilic malononitrile. Additionally, dialdehydes were employed effectively to produce bis poly-substituted pyrazoles in substantial quantities. The reaction was further explored with aldehydes containing electron-withdrawing substituents on the aromatic ring, and bulky aldehydes were converted to the desired products with relative ease. The applicability of the reaction was enhanced by investigating the use of heteroaryl aldehydes.

Experimental results demonstrated that aliphatic aldehydes were ineffective in this one-pot, catalyst-free reaction, primarily due to their lower reactivity towards nucleophilic addition compared to aromatic aldehydes. Scheme 1 illustrates the selective synthesis of 5-amino-1,3-diphenyl-1H-pyrazole-4-carbonitrile, indicating the potential for in situ preparation of these derivatives through the condensation of aromatic aldehyde, phenylhydrazine, and highly reactive malononitrile.

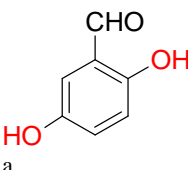
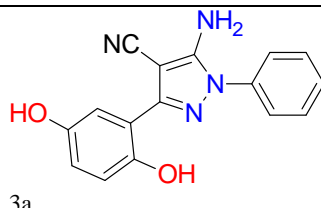
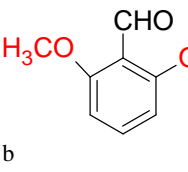
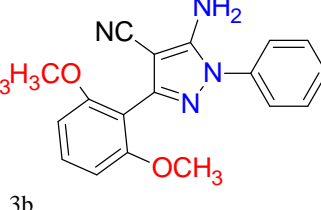
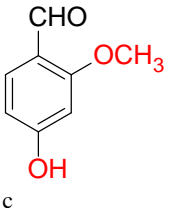
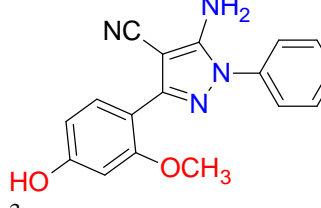
The method provides robust empirical evidence supporting its efficiency, with a BuniumPersicum extracted CoO-NPscatalyst reaction achieving high selectivity and minimal

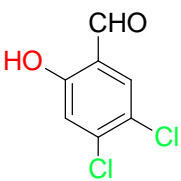
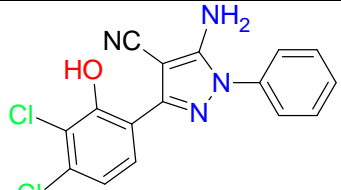
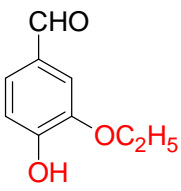
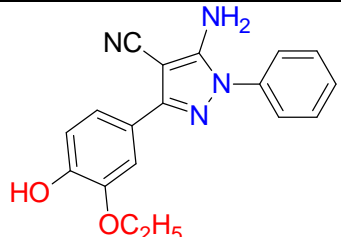
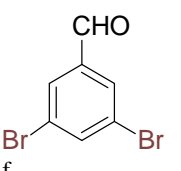
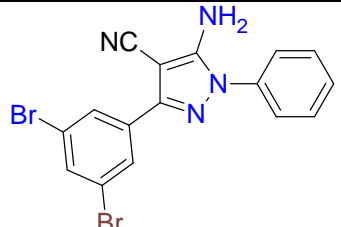
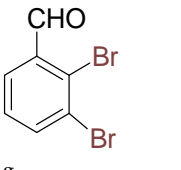
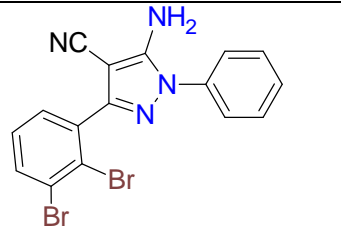
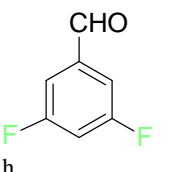
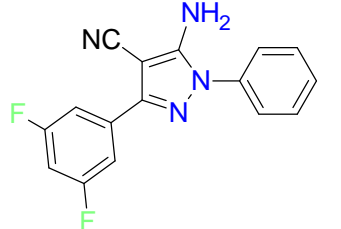
atom waste. To our knowledge, this method represents the first instance of conducting a 3-component pot synthesis-type reaction, ring closure, and subsequent aromatization within a single vessel BuniumPersicum extracted CoO-NPs a catalyst.

Spectroscopic analyses confirmed the structures of 5-amino-1,3-diphenyl-1H-pyrazole-4-carbonitrile derivatives. FT-IR spectra of compounds 3a, 3c, and 3d exhibited a broad band in the range of 3444-3322 cm^{-1} corresponding to the $\nu(\text{O-H})$ stretching of the aromatic hydroxyl group⁵⁶. For compound 3a, the (O-H) group was indicated by bands at 2952 and 1441 cm^{-1} ⁵⁷. The infrared spectra of compounds 3a-3j displayed bands between 3350-2953 cm^{-1} , attributed to the $\nu(\text{N-H})$ stretching of grafted amine groups⁵⁸. Additionally, the FT-IR spectra of all synthesized compounds revealed C=N stretching vibration bands between 1684 and 1545 cm^{-1} ⁵⁹.

In the ^1H NMR spectra of compounds 3a, 3c, 3d, and 3e (CDCl_3 , 500 MHz), the presence of an aromatic -OH group was indicated by a singlet at δ 5.84-11.78⁶⁰. The phenyl ring displayed a doublet in the range of δ 6.73 to 7.96, while the NH_2 group appeared as a 2H singlet between δ 7.34 and 8.20⁶¹. The methoxy group attached to the aromatic ring produced another singlet in the region δ 1.54-4.01⁶².

Table 1: Yield, color, reaction time, and physical constants of the product (3a-j)

Entry	Substrate	Product	Temp (°C)	Time ^a (min)	Yield (%)	TON	TOF (h^{-1})
3a			178	1.50	91.17	1.90	144.5
3b			127	2.00	94.99	1.85	99.2
3c			155	2.50	93.61	1.70	11.6

3d	 d	 3d	161	2.00	90.00	1.60	124.0
3e	 e	 3e	170	1.50	90.36	1.90	90.5
3f	 f	 3f	177	3.00	95.00	1.80	95.7
3g	 g	 3g	195	2.25	94.00	1.70	88.3
3h	 h	 3h	149	1.75	93.57	1.85	122.2

3i	 i	 3i	150	2.75	91.85	1.76	136.7
3j	 j	 3j	168	2.25	90.51	1.88	127.5

TLC was used to monitor the reaction at 80°C and 100°C until all of the aldehyde and acetophenone were consumed. b Isolated yield with a standard deviation of 2% following column chromatography.

Table 2: CoO-NPs catalyst recycling potential

No of cycle	Run 1	Run 2	Run 3	Run 4	Run 5
Yield (%)	95	92	90	87	83
Time(min)	2.00	2.00	2.00	2.00	2.00
TON	1.60	1.55	1.51	1.48	1.44
TOF	124.0	122.9	121.0	119.3	117.4

Table 3: CoO-NPs catalyst for the preparation of 5-amino-1,3-diphenyl-1H-pyrazole-4-carbonitrile derivatives

Sr. No	Catalyst	Time (min)	Temperature	Yield(%)	Reference
1	BF ₃ -Et ₂ O/ Dioxane	15	Room temperature	90	[22]
2	I ₂ -Al ₂ O ₃ (neutral)	1.5	M. W. (300W)60°C	95	[23]
3	NH ₄ Cl/ Solvent free	3	M.W. (480W)	95	[24]
4	BiCl ₃ /Solvent free	20	140°C	85	[25]
5	Phosphonium Ionic Liquid	150	145°C	80	[23]
6	CoO-NPs catalyst	2.0	100°C	95	Present work

We examined the reaction conditions with and without the CoO-NPs catalyst, as illustrated in Figures 1 and 2 and supported by X-ray diffraction (XRD) analyses (Table 1). Substituted benzaldehyde, malononitrile, and phenyl hydrazine were subjected to microwave irradiation at 100°C with 40% power (400 W maximum output) in a minimum solvent environment. For control experiments, all other parameters were maintained constant. Reactions conducted at 80 and 100°C without a catalyst resulted in no product formation (Table 1, entries 1-2). The optimal reaction conditions were identified as 1.5 minutes of microwave irradiation at 100°C with 5 mol% CoO-NPs catalyst, achieving a 95% yield (Table 1). Subsequent reactions using malononitrile, phenylhydrazine, and substituted aldehydes demonstrated that electron-donating and withdrawing substituents on the aryl ring were well-tolerated, with yields ranging from 90% to 95%, indicating substantial effectiveness. The synthesized compounds were characterized using ¹H NMR and FTIR analyses, with results comparable to those of commercially available compounds (Scheme 1).

To assess the recyclability of the CoO-NPs, we performed additional experiments using substituted benzaldehyde, malononitrile, and phenylhydrazine. The catalyst was recovered by filtration, washed with a hot water/ethanol mixture to remove any absorbed products, and then reused. As shown in Table 2, the catalyst maintained its catalytic activity across five recycling cycles, with yields consistently around 90%, 87%, 85%, 95%, 92%, 89%, 94%, 95%, 90%, and 85%, respectively. Further XRD analyses confirmed the catalyst's structural integrity after the fifth cycle (Figure 3). Additional characterization through energy-dispersive X-ray analysis (EDAX) and X-ray powder diffraction (XRD) confirmed that the *Sterculia* catalyst's activity, shape, and size distribution remained unchanged after five uses. Adsorption-desorption studies of nitrogen molecules provided further validation.

The proposed mechanism suggests that the CoO-NPs catalyst facilitates the activation of the aldehyde, which then reacts with the enol form of the ketone to form the concentrated product. 5-amino-1,3-diphenyl-1H-pyrazole-4-carbonitrile and their derivatives (Scheme 1) are produced by the elimination of a single water molecule from the condensed product.

ANTIMICROBIAL ACTIVITY

The newly synthesized compounds were assessed for their antibacterial and antifungal efficacy against a range of bacterial and fungal strains using the broth microdilution method. The test strains included Gram-positive bacteria such as *Staphylococcus aureus* (MCC 2010) and *Bacillus subtilis* (MCC 2010), as well as Gram-negative bacteria like *Escherichia coli* (MCC 2412) and *Pseudomonas aeruginosa* (MCC 2080). For bacterial testing, all isolates were cultured in nutritional broth at 37°C for 24 hours. Fungal spore suspensions were prepared using Tween 80 from 7-day-old fungal cultures grown on Sabouraud dextrose agar at 25°C. The final optical densities (ODs) of bacterial and fungal inocula were 0.2–0.3 and 0.5, respectively. Stock solutions were prepared with DMSO, and the concentrations measured were unaffected by the solvent. The minimum inhibitory concentration (MIC) for bacteria and fungi was determined to be 1000 µg/mL. Control agents such as fluconazole and streptomycin were employed for comparison.

Antibacterial and antifungal activities were evaluated following incubation at 37°C for 24 hours and at 25°C for 48 hours, respectively. Streptomycin, a broad-spectrum antibiotic, was the reference treatment, showing a minimum inhibitory concentration (MIC) of 10 mg/mL. The inhibition zones for streptomycin ranged from 12–16 mm for *E. coli* (MCC 2412), 10–12 mm for *B. subtilis* (MCC 2010), 12–15 mm for *P. aeruginosa* (MCC 2080), and 9–13 mm for *S. aureus* (MCC 2010). Compound 3a exhibited greater activity against *S. aureus* than other bacterial species. Compound 3e demonstrated superior effectiveness (19 mm inhibition zone) compared to the reference drug. In contrast, compound 3d showed reduced efficacy against *P. aeruginosa* compared to the standard antibiotic. Compound 3j was identified as the most potent against *E. coli*.

For antifungal evaluation, the standard drug fluconazole, with an MIC of 50 µg/mL, showed inhibition zones of 8–17 mm for *Candida albicans* (MCC 1439) and 10–17 mm for *Saccharomyces cerevisiae* (MCC 1033). The newly synthesized compounds exhibited greater activity than fluconazole, with a minimum inhibitory concentration (MIC) of 54 µg/mL for both fungal strains, indicating enhanced efficacy over the gold standard.

Table4: Antibacterial activities of the product (3a-j)

Compound	S. aureus	B. subtilis	E. coli	P. aeruginosa
3a	12	10	15	12
3b	10	12	12	15
3c	9	11	13	13
3d	13	10	14	14
3e	11	12	16	15
3f	12	11	12	12
3g	11	10	15	14
3h	12	12	13	12
3i	13	10	16	15
3j	12	11	15	11
Std	12	11	12	12

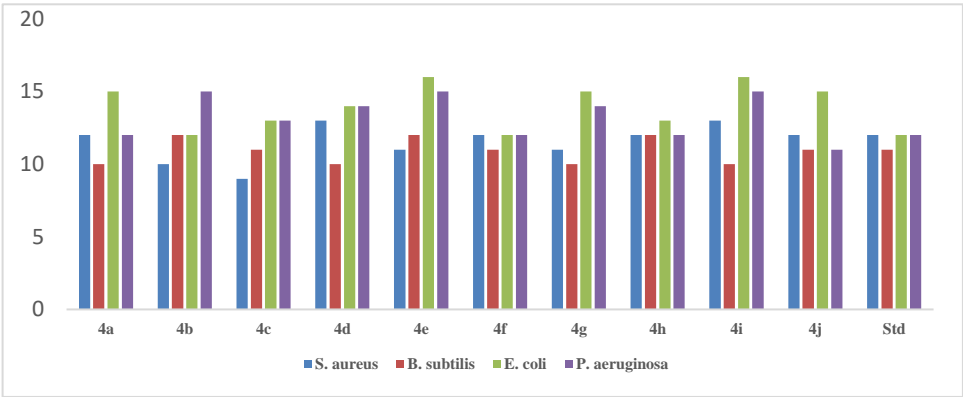


Figure 1: Antibacterial activities of the product (3a-j)

Table5: Antifungal activities of the product (3a-j)

Compound	Candida albicans	Saccharomyces cerevisiae
3a	16	11
3b	10	15
3c	13	16
3d	14	13
3e	8	15
3f	10	12
3g	9	13
3h	8	16
3i	17	17
Fluconazole	15	11

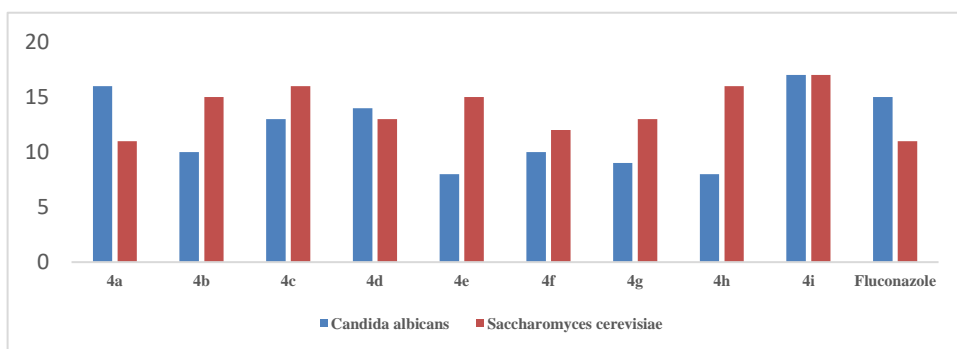


Figure 2: Antifungal activities of the product (3a-j)

4. Conclusion:

The study demonstrates that CoO nanoparticles exhibit a face-centered cubic structure and a spherical morphology, as confirmed by X-ray Diffraction (XRD) and Scanning Electron Microscopy (SEM) images. The elemental purity of the nanoparticles' composition is further validated by Energy-Dispersive X-ray Spectroscopy (EDAX) analysis. Using a multicomponent reaction approach, we have successfully developed a one-step synthesis method for poly-substituted amino pyrazole analogs. This process yields high-quality results rapidly, achieving good to excellent yields with the requirement for a CoO-NPs catalyst. Notably, this method offers several advantages, including simplified experimental procedures and the absence of hazardous by-products. The described procedure necessitates the use of CoO-NPs catalysts, toxic organic solvents, or dehydration processes, thus presenting an environmentally friendly strategy for the synthesis of pyrazole derivatives.

Acknowledgments

The Head of the Central Instrumentation Facility at the Savitribai Phule Pune University, Pune provided the spectra analysis.

Conflict of Interest

None.

References

1. Nikam, A. V.; Prasad, B. L. V.; Kulkarni, A. A. Wet chemical synthesis of metal oxide nanoparticles: a review. *CrystEngComm*. 2018, 20(35), 5091-5107.
2. Jeevanandam, J.; Kiew, S. F.; Boakye-Ansah, S.; Lau, S. Y.; Barhoum, A.; Danquah, M. K.; Rodrigues, J. Green approaches for the synthesis of metal and metal oxide nanoparticles using microbial and plant extracts. *Nanoscale*, 2022, 14(7), 2534-2571.
3. Ishak, N. M.; Kamarudin, S. K.; Timmiati, S. N. Green synthesis of metal and metal oxide nanoparticles via plant extracts: an overview. *Mater. Res. Express*. 2019, 6(11), 112004.
4. Iravani, S.; Varma, R. S. Sustainable synthesis of cobalt and cobalt oxide nanoparticles and their

- catalytic and biomedical applications. *Green Chem.*2020, 22(9), 2643-2661.
5. Aadil, M.; Zulfiqar, S.; Sabeeh, H.; Warsi, M. F.; Shahid, M.; Alsafari, I. A.; Shakir, I. Enhanced electrochemical energy storage properties of carbon-coated Co₃O₄ nanoparticles-reduced graphene oxide ternary nano-hybrids. *Ceram. Int.*2020, 46(11), 17836-17845.
 6. Prabakaran, D. D. M.; Sadaiyandi, K.; Mahendran, M.; Sagadevan, S. Precipitation method and characterization of cobalt oxide nanoparticles. *Appl. Phys. A*.2017, 123, 1-6.
 7. Srinivasan, S. Y.; Paknikar, K. M.; Bodas, D.; Gajbhiye, V. Applications of cobalt ferrite nanoparticles in biomedical nanotechnology. *Nanomedicine*.2018, 13(10), 1221-1238.
 8. Samuel, M. S.; Madhumita, R.; John, J. A.; Selvarajan, E.; Patel, H.; Chander, P. S.; Soundarya, J.; Vuppala, S.; Balaji, R.; Chandrasekar, N. A Review on Green Synthesis of Nanoparticles and Their Diverse Biomedical and Environmental Applications. *Catalysts*2022, 12 (5), 459.
 9. Waris, A.; Din, M.; Ali, A.; Afridi, S.; Baset, A.; Khan, A. U.; Ali, M. Green fabrication of Co and Co₃O₄ nanoparticles and their biomedical applications: A review. *Open Life Sci.*2021, 16(1), 14-30.
 10. Godoy-Gallardo, M.; Eckhard, U.; Delgado, L. M.; de Roo Puente, Y. J.; Hoyos-Nogués, M.; Gil, F. J.; Perez, R. A. Antibacterial approaches in tissue engineering using metal ions and nanoparticles: From mechanisms to applications. *Bioact. Mater.*2021, 6(12), 4470-4490.
 11. Carrillo-Carrion, C.; Nazarenus, M.; Paradinas, S. S.; Carregal-Romero, S.; Almendral, M. J.; Fuentes, M.; Parak, W. J. Metal Ions in the Context of Nanoparticles toward Biological Applications. *Curr. Opin. Chem. Eng.*2014, 4, 88-96.
 12. Hung, Y. L.; Hsiung, T. M.; Chen, Y. Y.; Huang, Y. F.; Huang, C. C. Colorimetric Detection of Heavy Metal Ions Using Label-Free Gold Nanoparticles and Alkanethiols. *J. Phys. Chem. C*2010, 114 (39), 16329-16334.
 13. Böhme, S.; Baccaro, M.; Schmidt, M.; Potthoff, A.; Stärk, H. J.; Reemtsma, T.; Kühnel, D. Metal Uptake and Distribution in the Zebrafish (*Danio rerio*) Embryo: Differences Between Nanoparticles and Metal Ions. *Environ. Sci.: Nano*2017, 4 (5), 1005-1015.
 14. Ghosh, M.; Sampathkumaran, E. V.; Rao, C. N. R. Synthesis and Magnetic Properties of CoO Nanoparticles. *Chem. Mater.*2005, 17 (9), 2348-2352.
 15. Haase, F. T.; Bergmann, A.; Jones, T. E.; Timoshenko, J.; Herzog, A.; Jeon, H. S.; Cuenya, B. R. Size Effects and Active State Formation of Cobalt Oxide Nanoparticles During the Oxygen Evolution Reaction. *Nat. Energy*2022, 7 (8), 765-773.
 16. Chu, J.; Sun, G.; Han, X.; Chen, X.; Wang, J.; Hu, W.; Xu, P. Ultrafine CoO Nanoparticles as an Efficient Cocatalyst for Enhanced Photocatalytic Hydrogen Evolution. *Nanoscale*2019, 11 (33), 15633-15640.
 17. Urabe, A. A.; Aziz, W. J. Biosynthesis of Cobalt Oxide (Co₃O₄) Nanoparticles Using Plant Extract of *Camellia Sinensis* (L.) Kuntze and *Apium Graveolens* L. as the Antibacterial Application. *World News Nat. Sci.*2019, 24, 356-364.
 18. Pagar, T.; Ghotekar, S.; Pagar, K.; Pansambal, S.; Oza, R. A Review on Bio-Synthesized Co₃O₄ Nanoparticles Using Plant Extracts and Their Diverse Applications. *J. Chem. Rev.*2019, 1 (4), 260-270.
 19. Fatima, M.; Rehmat, S.; Hassan, M.; Baig, M. M.; Shazad, T.; Majeed, F. Cestrum Nocturnum Leaf Extract Assisted Biogenic Synthesis of CoO Nanoparticles and Their Application in Cationic Dyes Photodegradation. *J. Fac. Eng. Technol.*2023, 27 (1), 65-74.
 20. Singh, A. K. A Review on Plant Extract-Based Route for Synthesis of Cobalt Nanoparticles: Photocatalytic, Electrochemical Sensing and Antibacterial Applications. *Curr. Res. Green Sustain. Chem.*2022, 5, 100270.
 21. Chelliah, P.; Wabaidur, S. M.; Sharma, H. P.; Jweeg, M. J.; Majdi, H. S.; AL. Kubaisy, M. M. R.; Lai, W. C. Green Synthesis and Characterizations of Cobalt Oxide Nanoparticles and Their Coherent Photocatalytic and Antibacterial Investigations. *Water*2023, 15 (5), 910.
 22. Samuel, M. S.; Selvarajan, E.; Mathimani, T.; Santhanam, N.; Phuong, T. N.; Brindhadevi, K.;

- Pugazhendhi, A. Green Synthesis of Cobalt-Oxide Nanoparticle Using Jumbo Muscadine (*Vitis rotundifolia*): Characterization and Photocatalytic Activity of Acid Blue-74. *J. Photochem. Photobiol. B: Biol.*2020, 211, 112011.
23. Memon, S. A.; Hassan, D.; Buledi, J. A.; Solangi, A. R.; Memon, S. Q.; Palabiyik, I. M. Plant Material-Protected Cobalt Oxide Nanoparticles: Sensitive Electro-Catalyst for Tramadol Detection. *Microchem. J.*2020, 159, 105480.
24. Aigbe, U. O.; Osibote, A. O. Green Synthesis of Metal Oxide Nanoparticles, and Their Various Applications. *J. Hazard. Mater. Adv.*2024, 100401.
25. Iravani, S.; Varma, R. S. Sustainable Synthesis of Cobalt and Cobalt Oxide Nanoparticles and Their Catalytic and Biomedical Applications. *Green Chem.*2020, 22 (9), 2643-2661.
26. Singh, A. K. A Review on Plant Extract-Based Route for Synthesis of Cobalt Nanoparticles: Photocatalytic, Electrochemical Sensing and Antibacterial Applications. *Curr. Res. Green Sustain. Chem.*2022, 5, 100270.
27. Iqbal, J.; Abbasi, B. A.; Batool, R.; Khalil, A. T.; Hameed, S.; Kanwal, S.; Mahmood, T. Biogenic Synthesis of Green and Cost-Effective Cobalt Oxide Nanoparticles Using Geranium wallichianum Leaves Extract and Evaluation of In Vitro Antioxidant, Antimicrobial, Cytotoxic, and Enzyme Inhibition Properties. *Mater. Res. Express*2019, 6 (11), 115407.
28. Verma, S. K.; Panda, P. K.; Kumari, P.; Patel, P.; Arunima, A.; Jha, E.; Suar, M. Determining Factors for the Nano-Biocompatibility of Cobalt Oxide Nanoparticles: Proximal Discrepancy in Intrinsic Atomic Interactions at Differential Vicinage. *Green Chem.*2021, 23 (9), 3439-3458.
29. Iqbal, J.; Abbasi, B. A.; Batool, R.; Khalil, A. T.; Hameed, S.; Kanwal, S.; Mahmood, T. Biogenic Synthesis of Green and Cost-Effective Cobalt Oxide Nanoparticles Using Geranium wallichianum Leaves Extract and Evaluation of In Vitro Antioxidant, Antimicrobial, Cytotoxic, and Enzyme Inhibition Properties. *Mater. Res. Express*2019, 6 (11), 115407.
30. Saeed, S. Y.; Mazhar, K.; Raees, L.; Mukhtiar, A.; Khan, F.; Khan, M. Green Synthesis of Cobalt Oxide Nanoparticles Using Roots Extract of *Ziziphus Oxyphylla* Edgew Its Characterization and Antibacterial Activity. *Mater. Res. Express*2022, 9 (10), 105001.
31. Bansal, S.; Sharma, K.; Gautam, V.; Lone, A. A.; Malhotra, E. V.; Kumar, S.; Singh, R. A Comprehensive Review of *Buniumpersicum*: A Valuable Medicinal Spice. *Food Rev. Int.*2023, 39 (2), 1184-1202. <https://doi.org/10.3390/molecules25143188>.
32. Shahsavari, N.; Barzegar, M.; Sahari, M. A.; Naghdibadi, H. Antioxidant Activity and Chemical Characterization of Essential Oil of *Buniumpersicum*. *Plant Foods Hum. Nutr.*2008, 63, 183-188.
33. Majidi, Z.; Bina, F.; Kahkeshani, N.; Rahimi, R. *Buniumpersicum*: A Review of Ethnopharmacology, Phytochemistry, and Biological Activities. *Tradit. Integr. Med.*2020.
34. Talei, G. R.; Mosavi, Z. Chemical Composition and Antibacterial Activity of *Buniumpersicum* from West of Iran. *Asian J. Chem.*2009, 21 (6), 4749.
35. Abbasi, B.; Daniali, M.; Ramezani, H.; Derakhshande, M.; Ghiasvand, R. The Effect of *Buniumpersicum* on Gastrointestinal Symptoms and Inflammatory Mediators in Irritable Bowel Syndrome Patients.
36. Hassanzad Azar, H.; Taami, B.; Aminzare, M.; Daneshamooz, S. *Buniumpersicum* (Boiss.) B. Fedtsch: An Overview on Phytochemistry, Therapeutic Uses and Its Application in the Food Industry. *J. Appl. Pharm. Sci.*2018, 8 (10), 150-158.
37. Singh, S.; Kumar, V. Biology, Genetic Improvement and Agronomy of *Buniumpersicum* (Boiss.) Fedtsch.: A Comprehensive Review. *J. Appl. Res. Med. Aromat. Plants*2021, 22, 100304.
38. Bader, G. N.; Rashid, R.; Ali, T.; Hajam, T. A.; Kareem, O.; Mir, S. A.; Jan, I. Medicinal Plants and Their Contribution in Socio-Economic Upliftment of the Household in Gurez Valley (J&K). In *Edible Plants in Health and Diseases: Volume 1: Cultural, Practical and Economic Value*; Springer Nature Singapore: Singapore, 2022; pp 107-136.

39. Samandari-Bahraseman, M. R.; Ismaili, A.; Esmaeili-Mahani, S.; Ebrahimie, E.; Loit, E. Buniumpersicum Seeds Extract in Combination with Vincristine Mediates Apoptosis in MCF-7 Cells through Regulation of Involved Genes and Proteins Expression. *Anti-Cancer Agents Med. Chem.* 2024, 24 (3), 213-223.
40. Singh, S.; Kumar, V. Biology, Genetic Improvement and Agronomy of Buniumpersicum (Boiss.) Fedtsch.: A Comprehensive Review. *J. Appl. Res. Med. Aromat. Plants* 2021, 22, 100304.
41. Sofi, P. A.; Zeerak, N. A.; Singh, P. Kala Zeera (Buniumpersicum Bioss.): A Kashmirian High Value Crop. *Turk. J. Biol.* 2009, 33 (3), 249-258.
42. Singh, S.; Kumar, V. Biology, Genetic Improvement and Agronomy of Buniumpersicum (Boiss.) Fedtsch.: A Comprehensive Review. *J. Appl. Res. Med. Aromat. Plants* 2021, 22, 100304.
43. Hajimohammadi, B.; Raeisi, M.; Eftekhari, E.; Mohebat, R.; Saffari, A. Studying the Effect of Allium sativum and Buniumpersicum Essential Oils on Histamine Production in Mahyaveh, an Iranian Seasoned Fish Sauce. *J. Food Saf.* 2019, 39 (1), e12590.
44. Balouiri, M.; Sadiki, M.; Ibsouda, S. K. Methods for In Vitro Evaluating Antimicrobial Activity: A Review. *J. Pharm. Anal.* 2016, 6 (2), 71-79.
45. Finlay, J.; Miller, L.; Poupard, J. A. A Review of the Antimicrobial Activity of Clavulanate. *J. Antimicrob. Chemother.* 2003, 52 (1), 18-23.
46. Rios, J. L.; Recio, M. C. Medicinal Plants and Antimicrobial Activity. *J. Ethnopharmacol.* 2005, 100 (1-2), 80-84.
47. Nazzaro, F.; Fratianni, F.; Coppola, R.; De Feo, V. Essential Oils and Antifungal Activity. *Pharmaceuticals* 2017, 10 (4), 86.
48. Sortino, M.; Delgado, P.; Juárez, S.; Quiroga, J.; Abonía, R.; Insuasty, B.; Zacchino, S. A. Synthesis and Antifungal Activity of (Z)-5-Arylidenerhodanines. *Bioorg. Med. Chem.* 2007, 15 (1), 484-494.
49. Ghosh, M.; Sampathkumaran, E. V.; Rao, C. N. R. Synthesis and Magnetic Properties of CoO Nanoparticles. *Chem. Mater.* 2005, 17 (9), 2348-2352.
50. Al-Fakeh, M. S.; Alsaedi, R. O. Synthesis, Characterization, and Antimicrobial Activity of CoO Nanoparticles from a Co(II) Complex Derived from Polyvinyl Alcohol and Aminobenzoic Acid Derivative. *Sci. World J.* 2021, 2021 (1), 6625216.
51. Horká, V.; Civiš, S.; Špirko, V.; Kawaguchi, K. The Infrared Spectrum of CN in Its Ground Electronic State. *Collect. Czechoslov. Chem. Commun.* 2004, 69 (1), 73-89.
52. Shibahara, T.; Mori, M. Raman and Infrared Spectra of MU.-O₂ Dicobalt (III) Complexes. *Bull. Chem. Soc. Jpn.* 1978, 51 (5), 1374-1379.
53. He, X.; Song, X.; Qiao, W.; Li, Z.; Zhang, X.; Yan, S.; Du, Y. Phase- and Size-Dependent Optical and Magnetic Properties of CoO Nanoparticles. *J. Phys. Chem. C* 2015, 119 (17), 9550-9559.
54. Ye, Y.; Yuan, F.; Li, S. Synthesis of CoO Nanoparticles by Esterification Reaction under Solvothermal Conditions. *Mater. Lett.* 2006, 60 (25-26), 3175-3178.
55. Allaadini, G.; Muhammad, A. Study of Influential Factors in Synthesis and Characterization of Cobalt Oxide Nanoparticles. *J. Nanostruct. Chem.* 2013, 3, 1-16.
56. Smidt, E.; Meissl, K. The Applicability of Fourier Transform Infrared (FT-IR) Spectroscopy in Waste Management. *Waste Manage.* 2007, 27 (2), 268-276.
57. Antsiferov, V. N.; Gilyov, V. G.; Karmanov, V. I. IR-Spectra and Phases Structure of Sialons. *Vibr. Spectrosc.* 2002, 30 (2), 169-173.
58. Norbutayevich, N. U.; Nurmuminovich, F. N.; Turovovich, A. D. The Study of the IR Spectra of Technopolises Modifiers. *Aust. J. Tech. Nat. Sci.* 2019, (7-8), 80-86.
59. Lussier, L. S.; Sandorfy, C.; LE-Thanh, H. O.; Vocelle, D. The Effect of Acids on the Infrared Spectra of Schiff Bases—II. Imines Containing the C=C-N AND C=C-C=N Units.

- Photochem. Photobiol.1987, 45, 801-808.
60. Hoffman, R. A.; Forsén, S.; Gestblom, B. Analysis of NMR Spectra: A Guide for Chemists; Vol. 5; Springer Science & Business Media, 2012.
61. Samsonowicz, M.; Hrynaskiewicz, T.; Świsłocka, R.; Regulska, E.; Lewandowski, W. Experimental and Theoretical IR, Raman, NMR Spectra of 2-, 3- and 4-Aminobenzoic Acids. J. Mol. Struct.2005, 744, 345-352.
62. Stevenson, P. J. Second-order NMR Spectra at High Field of Common Organic Functional Groups. Org. Biomol. Chem.2011, 9 (7), 2078-2084.